Improved Photovoltaic Performance of PPV-Based Copolymers Using Optimized Fullerene-Based Counterparts

Pavel A. Troshin, Olga A. Mukhacheva, Özlem Usluer, Andrey E. Goryachev, Alexander V. Akkuratov, Diana K. Susarova, Nadezhda N. Dremova, Silke Rathgeber, Niyazi Serdar Sariciftci, Vladimir F. Razumov, and Daniel A. M. Egbe*

Organic polymer-based bulk heterojunction solar cells have been intensively developed during the last decade. Historically, conjugated polymers of the PPV (para-phenylene vinylene) family such as poly(2-[(3'-7'-dimethyloctyl)oxy]-5-methoxy-1,4-phenylene}-1,2-ethenediyl) (MDMO-PPV) and poly({[(2-ethylhexyl)oxy]-5-methoxy-1,4-phenylene}-1,2-ethenediyl) (MEH-PPV) were among the very first electron-donor materials utilized for the construction of plastic solar cells. Power-conversion efficiencies up to 2.5–3.0% have been obtained for solar cells based on the blends of fullerene derivatives [6,6]-phenyl-C_{61}-butyric acid methyl ester ([60]PCBM) and [6,6]-phenyl-C_{71}-butyric acid methyl ester ([70]PCBM), and MDMO-PPV.[1,2]

Poly(3-alkylthiophenes) (P3ATs) formed the next generation of electron-donor polymers and were shown to be more promising compared with PPVs.[3] Bulk-heterojunction solar cells based on composites of poly(3-hexylthiophene) (P3HT) with [60]PCBM have demonstrated reproducible power-conversion efficiencies of 3.5–4.5%.[4,5] The P3HT/PCBM composite system has been a "running horse" in organic photovoltaics for many years.[6]

The emergence of third-generation electron-donor copolymers has led to significant progress in organic photovoltaics.[7,8] Polymer-based solar cells with efficiencies of 5–7% have been reported recently by many research groups worldwide.[9–11] Record performances were achieved using so-called "push-pull" polymers comprising different electron-deficient heterocyclic blocks such as quinoxaline[12] benzothiadiazole,[13] 1,4-diketopyrrolopyrrole,[14] thieno[3,4-b]thiophene,[15] thieno[3,4-c]pyrrole-4,6-dione,[16,17] and isoindigo[17] in combination with electron-rich thiophene units or thiophene-based heterocycles such as cyclopentadithiophene,[18] dithienobenzene,[19] or dithienosilole.[20] These examples give the impression that the presence of both electron-deficient heterocycles and electron-donating thiophene rings in the polymer structure is an essential requirement for achieving a high photovoltaic performance[7–11]

This communication features an alternative type of conjugated polymer that can produce competitive photovoltaic characteristics compared with modern "push-pull" polymer systems. The investigated polymer, **AnE-PV*stat*** (**Figure 1**), is distinguished by its PPV-type molecular structure, the absence of any heterocyclic units, particularly thiophene rings, and the presence of an anthracene unit bearing two adjacent triple bonds. Another peculiarity of this polymer is the statistical distribution of n-octyloxy- and 2-ethylhexyloxy-solubilizing side chains along the polymer backbone.[21] Solar cells based on the polymer **AnE-PV*stat*** and the conventional fullerene-based material [60]PCBM showed rather modest power-conversion efficiencies of 2.0–3.0% under our experimental conditions. However, the photovoltaic performance of **AnE-PV*stat*** was improved significantly to the level of ≈4.3% when specially designed fullerene derivatives **F3** and **F11** were applied instead of [60]PCBM. The observed strong effect of the fullerene component points to the need for the simultaneous development of electron-donor polymers and electron-acceptor fullerene derivatives on the way towards efficient organic photovoltaics.

A family of anthracene-containing PPV-PPE polymers was designed a long time ago and has been explored intensively in organic solar cells in combination with conventional fullerene-based materials such as [60]PCBM and [70]PCBM.[22–24] A very low molecular weight version of **AnE-PV*stat*** (LMW-**AnE-PV*stat***, M_w = 8460 g mol^{-1}, PDI = 2.2) was studied in detail very recently.[25] In that previous work, we combined LMW-**AnE-PV*stat*** with seventeen different fullerene derivatives, while investigating the photovoltaic behavior of this polymer. Solar cells based on LMW-**AnE-PV*stat***:[60]PCBM yielded power-conversion efficiencies of ≈2.5%. Interestingly, composites of the polymer with a few other fullerene derivatives have demonstrated enhanced photovoltaic performances exceeding 3.0%. It is notable that the solar cells showed high open-circuit voltages due to the high oxidation potential of the **AnE-PV*stat*** polymer,

Dr. P. A. Troshin, O. A. Mukhacheva,
Dr. A. E. Goryachev, A. V. Akkuratov, Dr. D. K. Susarova,
Dr. N. N. Dremova, Prof. V. F. Razumov
Institute for Problems of Chemical Physics
of Russian Academy of Sciences, Semenov Prospect 1
Chernogolovka, 142432, Russian Federation
E-mail: troshin2003@inbox.ac.ru
Dr. Ö. Usluer, Prof. N. S. Sariciftci, Dr. D. A. M. Egbe
Linz Institute for Organic Solar Cells (LIOS)
Physical Chemistry
Johannes Kepler University Linz
Altenberger Straße 69, Linz, A-4040, Austria
Dr. Ö. Usluer
Department of Chemistry
Mugla University
Kotekli, 48000 Mugla, Turkey
Prof. S. Rathgeber
University Koblenz-Landau
Institute for Natural Sciences
Universitätsstrasse 1, Koblenz, 56060, Germany

DOI: 10.1002/aenm.201200118

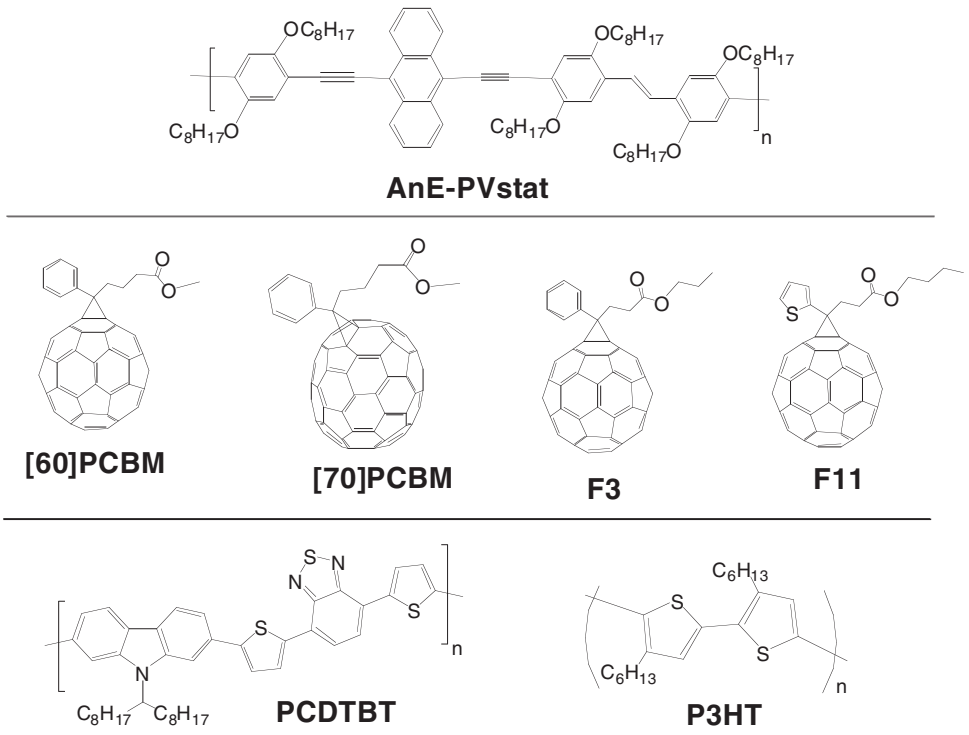

Figure 1. Molecular structures of the investigated materials.

corresponding to its deep-lying highest-occupied-molecular-orbital (HOMO) energy level.[24]

A new version of **AnE-PV*stat***, possessing an improved molecular weight (M_w = 19 300 g mol^{-1}), was applied in this work. This polymer sample is characterized by rather high polydispersity (PDI = 2.8) arising from the presence of low-molecular-weight components (see GPC profile, Supporting Information). Guided by the results of our previous studies, we investigated the performance of **AnE-PV*stat*** in organic bulk-heterojunction solar cells in combination with a few different fullerene derivatives. The range of studied fullerene derivatives included compounds **F3**, **F11** and the references [60]PCBM and [70]PCBM (Figure 1).

Organic bulk-heterojunction solar cells with the classical architecture of indium tin oxide (ITO)/poly(3,4-ethylenedioxy thiophene):poly(styrenesulfonate) (PEDOT:PSS)/**AnE-PV*stat***:fullerene-derivative composite/Ca (20 nm)/Ag (100 nm) were fabricated. The polymer and the fullerene derivatives were mixed in the weight ratio of 1:2 (w/w), which is similar to the 1:1.8 (w/w) component ratio used in the previous study.[24] The photovoltaic characteristics of the devices obtained from the *I*–*V* measurements are presented in **Table 1**. It is seen from the table that the conventional fullerene-based materials, [60]PCBM and [70]PCBM, showed rather modest (<3.0%) performances when used in combination with **AnE-PV*stat***.

The application of the fullerene derivatives **F3** and **F11** instead of [60]PCBM and [70]PCBM improved the photovoltaic performance of **AnE-PV*stat*** dramatically. Power-conversion efficiencies of 4.3% (values corrected for the true AM1.5 spectrum (non-corrected values were about 5.0%)) (Table 1) were reached for the devices comprising **F3** and **F11**. It should be noted that these values were highly reproducible; the efficiencies between 4.0 and 4.3% were reached for approximately 85–90% of the devices in series. The improved performance of the devices comprising **F3** and **F11** is well illustrated by the *I*–*V* curves shown in **Figure 2**.

It is notable that the electronic properties of both compound **F3** and **F11** are very similar to that of [60]PCBM. In particular, the first reduction potentials of all four of the studied fullerene derivatives (including [70]PCBM) were equal to each other within experimental error (10–20 mV, Table S1). Therefore, the observed different photovoltaic performances of the composites of these fullerene derivatives with **AnE-PV*stat*** cannot be ascribed to the improved electronic properties of **F3** and **F11** compared with [60]PCBM and [70]PCBM. This conclusion also

Table 1. Characteristics of photovoltaic cells based on **AnE-PV*stat*** and the different fullerene derivatives.

Fullerene derivative	V_{OC} [mV]	I_{SC}[a)] [mA cm^{-2}]	FF [%]	η[a)] [%]
[60]PCBM	870	8.0 (6.8)	49	3.4 (2.9)
[70]PCBM	809	6.8 (5.9)	44	2.4 (2.1)
F3	822	9.3 (8.0)	65	5.0 (4.3)
F11	860	9.7 (8.2)	60	5.0 (4.2)

[a)]The I_{SC} and η values obtained under simulated solar irradiation (100 mW cm^{-2}) are provided. The I_{SC} and η values corrected for the spectral mismatch between the simulated solar irradiation and true AM1.5 conditions are given in brackets.

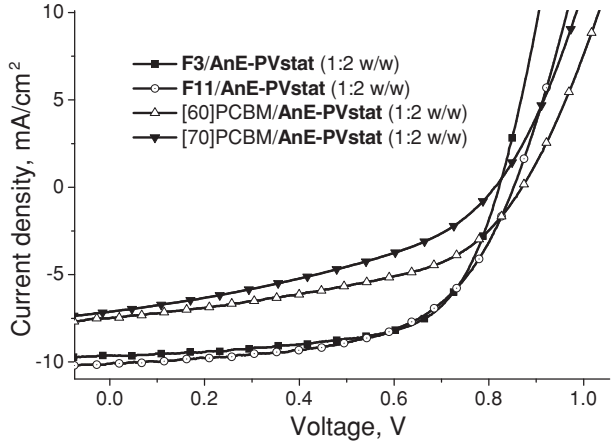

Figure 2. *I–V* curves of photovoltaic devices based on the different fullerene derivatives and **AnE-PV*stat*** (simulated AM1.5 irradiation, 100 mW cm^{-2}).

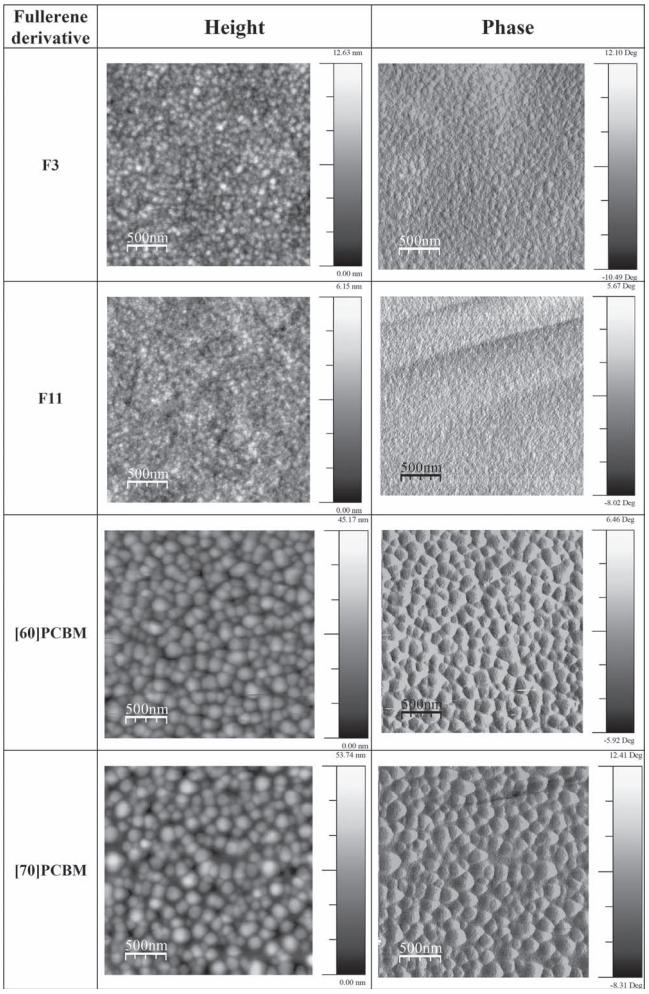

Figure 3. The height and phase AFM topography images of the composites of **AnE-PVstat** with the different fullerene derivatives in a 1:2 w/w ratio.

agrees with the device characteristics shown in Table 1, since the open-circuit voltages (V_{OC}) do not increase going from [60]PCBM to **F3** or **F11**.

The devices comprising **F3** and **F11** blended with **AnE-PV*stat*** demonstrated enhanced short-circuit current densities and, most importantly, they showed significantly improved fill factors (Table 1). Optical absorption spectra recorded for the pure fullerene derivatives **F3**, **F11**, and [60]PCBM (Figure S2) and their composites with **AnE-PV*stat*** (Figure S3) reflected no significant changes when going from one fullerene derivative to the other. Therefore, the higher current densities obtained for the devices comprising **F3** and **F11** cannot be explained by improved light harvesting in these systems.

The increased fill factors and current densities imply that the blends of **AnE-PV*stat*** with **F3** and **F11** possess improved active-layer morphologies. This suggestion is supported by the AFM topography images of the blends shown in **Figure 3**. The films comprising [60]PCBM and [70]PCBM exhibited characteristic grain-type structures on the surface that vary in size from 100 to 250 nm. Most probably, these grains correspond to the clusters comprising predominantly only one material (polymer or fullerene derivative),[26] thus implying rather strong phase separation between the components of the composites.

It is also known that the exciton diffusion lengths in organic semiconductors typically do not exceed 20 nm.[27] Therefore, the formation of larger clusters in the blends of **AnE-PV*stat*** with [60]PCBM and [70]PCBM leads to significant recombination losses that decrease the short-circuit current densities. The unbalanced active-layer morphology also damages charge transport to the electrodes and lowers the fill factors of the devices. Therefore, the less-favorable nanoscale morphology of the blends of **AnE-PV*stat*** with [60]PCBM and [70]PCBM explains their comparatively lower photovoltaic performance.

The blends of **AnE-PV*stat*** with **F3** and **F11** produced much more homogeneous films compared with the systems comprising [60]PCBM and [70]PCBM. The best-performing **F3**/**AnE-PV*stat*** and **F11**/**AnE-PV*stat*** composites revealed tiny grains on the film surface whose size vary in the range of 15–30 nm. These values are quite close to the typical exciton diffusion lengths in organic semiconductors.[26] Therefore, one might assume that the nanoscale morphology of these two blends is well-balanced, which corroborates well with their superior photovoltaic performance.

Additional proof of the large-scale phase separation between the fullerene and the polymer components in the blends of **AnE-PV*stat*** with [60]PCBM and [70]PCBM was obtained using scanning electron microscopy (SEM). The SEM images obtained for the **AnE-PV*stat***:[60]PCBM and **AnE-PV*stat***:[70]PCBM composites revealed round-shaped features approaching 150 and 300 nm in size, respectively (**Figure 4**). On the contrary, no large clusters were detected in the blends of **AnE-PV*stat*** with **F3** and **F11** by SEM, which proves that the polymer and the fullerene derivatives were better intermixed in these composites.

The results described above point to the existence of some correlation between the photovoltaic performance of the **AnE-PV*stat***: fullerene-derivative composites on the one hand, and the topology of their films revealed by the AFM measurements on the other. This correlation is visualized graphically in **Figure 5**. It is seen from this figure that both the fill factor and

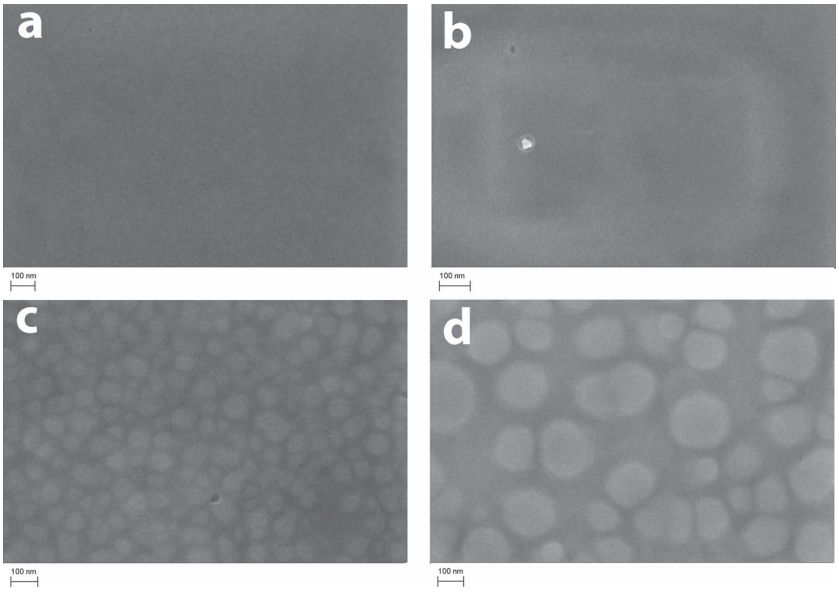

Figure 4. a–d) SEM images for the composites of **AnE-PV*stat*** with the different fullerene derivatives mixed in a 1:2 w/w ratio: **AnE-PV*stat*:F3** (a), **AnE-PV*stat*:F11** (b), **AnE-PV*stat*:**[60]PCBM (c) and **AnE-PV*stat*:**[70]PCBM (d).

the power-conversion efficiency of the devices depend strongly on the average lateral size of the grains extracted from the AFM images. It is notable also that the short-circuit current of the devices follows the same trend (Figure S4). The right part of the plot corresponds to the systems that are characterized by grain sizes above 100 nm. This area is populated by points corresponding to the **AnE-PV*stat*:**[60]PCBM and **AnE-PV*stat*:**[70]PCBM composites, which showed rather modest photovoltaic parameters (both FF and η). The left part of the graph corresponds to the **AnE-PV*stat*:F3** and **AnE-PV*stat*:F11** composites, which showed a fine film structure (grain size < 30 nm) and a high photovoltaic performance. This image illustrates quite well the advantages of using the fullerene derivatives **F3** and **F11** instead of [60]PCBM and [70]PCBM. Most probably, the improved morphology of the blends comprising **F3** and **F11** is related to the enhanced compatibility of these fullerene derivatives with the polymer. Similar effects have been reported recently for a number of composites of [70] fullerene derivatives with MDMO-PPV and P3HT.[28]

Most probably, some variations in the chemical structure of the fullerene derivatives, particularly, the appearance of longer and non-branched alkyl chains attached to the carboxylic groups in **F3** and **F11**, alter the kinetics and, perhaps also the thermodynamics of the film-formation process. In other words, some intermolecular interactions between the fullerene-derivative (**F3** or **F11**) and the polymer (**AnE-PV*stat***) components of the blend affect the film-formation process and prevent large-scale phase separation. This aspect will be addressed in more detail in a subsequent study. A systematic investigation of >200 different fullerene/polymer composites and a deeper discussion of the material compatibility issue is reported elsewhere.[29]

The high photovoltaic performance of the non-optimized devices based on **AnE-PV*stat*** and the **F3** and **F11** fullerene derivatives suggests that the polymer presented in this work is a rather promising material. We intentionally compared **AnE-PV*stat*** with P3HT (which has been a "running horse" in organic photovoltaics for years)[6] and the conjugated copolymer PCDTBT (Poly[[9-(1-octylnonyl)-9H-carbazole-2,7-diyl]-2,5-thiophenediyl-2,1,3-benzothiadiazole-4,7-diyl-2,5-thiophenediyl])[30,31] (Figure 1). The obtained characteristics of solar cells comprising P3HT and PCDTBT as conjugated polymers, and **F3**, **F11**, and [60]PCBM as [60]fullerene derivatives are listed in **Table 2**. It is seen from these data that the best performances were produced by the systems comprising [60]PCBM as

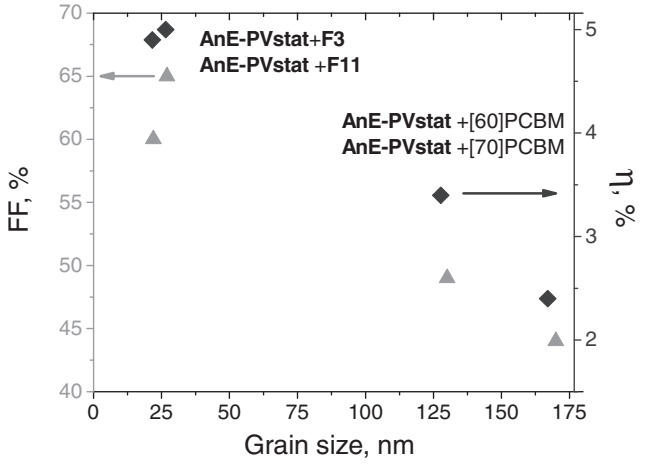

Figure 5. The correlation between the photovoltaic parameters of the **AnE-PV*stat*:**fullerene-derivative blends obtained under simulated solar irradiation (100 mW cm^{-2}) and the topology of their films revealed by AFM measurements (grain size).

Table 2. Characteristics of photovoltaic cells based on P3HT, PCDTBT, and the different [60]fullerene derivatives.

Fullerene derivative	V_{OC} [mV]	I_{SC}[a)] [mA cm^{-2}]	FF [%]	η[a)] [%]
P3HT, (P3HT:fullerene ratio 1.75:1 w/w)				
[60]PCBM	640	10.6 (9.1)	55	3.7 (3.2)
F3	550	9.3	43	2.2
F11	600	10.0	43	2.6
PCDTBT, (PCDTBT:fullerene ratio 1:4 w/w)				
[60]PCBM	805	9.5 (8.5)	57	4.4 (3.9)
F3	801	9.7 (8.7)	50	3.9 (3.5)
F11	780	10.4 (9.2)	51	4.1 (3.6)

[a)]The I_{SC} and η values obtained under simulated solar irradiation (100 mW cm^{-2}) are provided. The I_{SC} and η values corrected for the spectral mismatch between the simulated solar irradiation and true AM1.5 conditions are given in brackets.

the fullerene-based component. The composites of P3HT and PCDTBT with **F3** and **F11** showed comparable, but still inferior performances. These examples confirm that **F3** and **F11** do not possess any specific properties that would improve the photovoltaic performance of any conjugated polymer. It is more correct to think that **F3** and **F11** are optimal fullerene counterparts for the **AnE-PV*stat*** polymer, while [60]PCBM is optimal for P3HT and PCDTBT (simply because these polymers were selected via screening in combination with [60]PCBM). Historically, many novel and promising conjugated polymers have been abandoned because of their low (2–3%) performance in combination with [60]PCBM. The example of **AnE-PV*stat*** presented in this communication allows one to think that many of these previously abandoned polymers might show state-of-the-art performances if appropriate fullerene-based counterparts were provided. This conclusion is also supported by our systematic study of more than 200 different fullerene derivative/polymer systems.[31]

It is noteworthy that **AnE-PV*stat*** outperformed P3HT and the promising conjugated copolymer PCDTBT significantly, at least when studied in combination with [60]fullerene derivatives whose cost (in contrast to that of [70]fullerene derivatives) allows for commercial-scale applications. This result proves that the polymer-structure concept presented here might compete well with currently explored "push-pull" systems based one the combinations of electron-deficient and electron-rich heterocycles. At the same time, additional integration of push-pull chromophores into the **AnE-PV*stat*** polymer structure might also be an interesting direction in the design of novel low bandgap conjugated polymers for photovoltaic applications.

Experimental Section

General: All of the solvents and reagents were purchased from Sigma–Aldrich or Acros Organics and were used as received (acetone, toluene, isopropanol), or were purified by distillation (chlorobenzene, 1,2-dichlorobenzene). **AnE-PV*stat*** was obtained using the synthetic route described previously.[21] Poly(3-hexylthiophene) of EE grade was purchased from Rieke Metals company. The conjugated copolymer PCDTBT (M_w = 52 300 g mol^{-1}; PDI = 6.0) was synthesized using standard procedures previously reported in the literature.[8,32,33] The synthesis of the fullerene derivatives was performed according to a previously reported procedure.[34] The synthesis and spectroscopic characteristics of **F3** and **F11** have been reported previously.[35,36]

Fabrication of Photovoltaic Devices: The conjugated polymer **AnE-PV*stat*** (6.7 mg) and the fullerene derivative (13.4 mg) were dissolved together in 1 ml of chlorobenzene while stirring at room temperature for 12 h. The prepared solution was filtered through a 0.45 μm polytetrafluoroethylene (PTFE) syringe filter and was subjected to spin-coating at 900 rpm on top of annealed PEDOT:PSS films deposited on patterned ITO electrodes (a general description of the substrate preparation procedure is given by Troshin et al.[37]). The obtained films were transferred immediately into a vacuum chamber integrated inside an MBraum glovebox and pumped down for approximately 1 h until the pressure dropped below 4×10^{-6} mbar. The top electrode comprising Ca (20 nm) and Ag (100 nm) was deposited by thermal evaporation. The finalized devices were immediately subjected to *I–V* characterization.

Characterization of the Photovoltaic Devices: The current–voltage (*I–V*) characteristics of the devices were obtained in the dark and under simulated 100 mW cm^{-2} AM1.5 solar irradiation provided by a KHS Steuernagel solar simulator. The intensity of the illumination was checked every time before the measurements using a calibrated silicon diode with a known spectral response. The *I–V* curves were recorded using a Keithley 2400 source-measurement unit in a normal air atmosphere without applying any special encapsulation or protection to the photovoltaic devices. The incident photon-to-current efficiency (IPCE) spectra were measured using a specially designed setup, by LOMO Instruments, Russia.

Supporting Information

Supporting Information is available from the Wiley Online Library or from the author.

Acknowledgements

The authors acknowledge financial support provided by the Russian Ministry of Science and Education in the framework of the contract No. 02.740.11.0749, and by the Federal Program "Priority Directions of the Research and Development of the Scientific and Technological Infrastructure in Russia in 2007-2013", the Russian Foundation for Basic Research (10-03-00443a), the Russian President Science Foundation (MK-4916.2011.3), and the Deutsche Forschungsgemeinschaft (DFG) in the framework of SPP 1355.

Received: February 13, 2012
Published online: June 15, 2012

[1] S. E. Shaheen, C. J. Brabec, N. S. Sariciftci, F. Padinger, T. Fromherz, J. C. Hummelen, *Appl. Phys. Lett.* **2001**, *78*, 841.
[2] M. M. Wienk, J. M. Kroon, W. J. H. Verhees, J. Knol, J. C. Hummelen, P. A. van Hall, R. A. J. Janssen, *Angew. Chem. Int. Ed.* **2003**, *42*, 3371.
[3] F. Padinger, R. S. Rittberger, N. S. Sariciftci, *Adv. Funct. Mater.* **2003**, *13*, 85.
[4] P. Schilinsky, C. Waldauf, C. Brabec, *Adv. Funct. Mater.* **2006**, *16*, 1669.
[5] V. Shrotriya, G. Li, Y. Yao, T. Moriarty, K. Emery, Y. Yang, *Adv. Funct. Mater.* **2006**, *16*, 2016.
[6] M. T. Dang, L. Hirsch, G. Wantz, *Adv. Mater.* **2011**, *23*, 3597.
[7] Y.-J. Cheng, S.-H. Yang, C.-S. Hsu, *Chem. Rev.* **2009**, *109*, 5868.
[8] J. Chen, Y. Cao, *Acc. Chem. Res.* **2009**, *42*, 1709.
[9] R. F. Service, *Science* **2011**, *332*, 293.
[10] D. Gendron, M. Leclerc, *Energy Environ. Sci.* **2011**, *4*, 1225.
[11] J. M. Szarko, J. Guo, B. S. Rolczynski, L. X. Chen, *J. Mater. Chem.* **2011**, *21*, 7849.
[12] E. Wang, L. Hou, Z. Wang, S. Hellström, F. Zhang, O. Inganäs, M. R. Andersson, *Adv. Mater.* **2010**, *22*, 5240.
[13] D. Mühlbacher, M. Scharber, M. Morana, Z. Zhu, D. Waller, R. Gaudiana, C. Brabec, *Adv. Mater.* **2006**, *18*, 2884.
[14] M. M. Wienk, M. Turbiez, J. Gilot, R. A. J. Janssen, *Adv. Mater.* **2008**, *20*, 2556.
[15] Y. Liang, Y. Wu, D. Feng, S.-T. Tsai, H.-J. Son, G. Li, L. Yu, *J. Am. Chem. Soc.* **2009**, *131*, 56.
[16] C. Piliego, T. W. Holcombe, J. D. Douglas, C. H. Woo, P. M. Beaujuge, J. M. J. Frechet, *J. Am. Chem. Soc.* **2010**, *132*, 7595.
[17] T.-Y. Chu, J. Lu, S. Beaupré, Y. Zhang, J.-R. Pouliot, S. Wakim, J. Zhou, M. Leclerc, Z. Li, J. Ding, Y. Tao, *J. Am. Chem. Soc.* **2011**, *133*, 4250.
[18] E. Wang, Z. Ma, Z. Zhang, K. Vandewal, P. Henriksson, O. Inganäs, F. Zhang, M. R. Andersson, *J. Am. Chem. Soc.* **2011**, *133*, 14244.
[19] Y. Liang, Z. Xu, J. Xia, S.-T. Tsai, Y. Wu, G. Li, C. Ray, L. Yu, *Adv. Mater.* **2010**, *22*, E135.

[20] J. Hou, H.-Y. Chen, S. Zhang, G. Li, Y. Yang, *J. Am. Chem. Soc.* **2008**, *130*, 16144.
[21] D. A. M. Egbe, G. Adam, A. Pivrikas, A. M. Ramil, E. Birckner, V. Cimrova, H. Hoppe, N. S. Sariciftci, *J. Mater. Chem.* **2010**, *20*, 9726.
[22] D. A. M. Egbe, S. Türk, S. Rathgeber, F. Kühnlenz, R. Jadhav, A. Wild, E. Birckner, G Adam, A. Pivrikas, V. Cimrova, G. Knör, N. S. Sariciftci, H. Hoppe, *Macromolecules* **2010**, *43*, 1261.
[23] S. Rathgeber, D. Bastos de Toledo, E. Birckner, H. Hoppe, D. A. M. Egbe, *Macromolecules* **2010**, *43*, 306.
[24] D. A. M. Egbe, H. Neugebauer, N. S. Sariciftci, *J. Mater. Chem.* **2011**, *21*, 1338.
[25] D. K. Susarova, E. A. Khakina, P. A. Troshin, A. E. Goryachev, N. S. Sariciftci, V. F. Razumov, D. A. M. Egbe, *J. Mater. Chem.* **2011**, *21*, 2356.
[26] H. Hoppe, T. Glatzel, M. Niggemann, A. Hinsch, M. C. Lux-Steiner, N. S. Sariciftci, *Nano Lett.* **2005**, *5*, 269.
[27] P. W. M. Blom, V. D. Mihailetchi, J. A. Koster, D. E. Markov, *Adv. Mater.* **2007**, *19*, 1551.
[28] P. A. Troshin, H. Hoppe, A. S. Peregudov, M. Egginger, S. Shokhovets, G. Gobsch, N. S. Sariciftci, V. F. Razumov, *ChemSusChem* **2011**, *4*, 119.
[29] P. A. Troshin, D. K. Susarova, E. A. Khakina, A. E. Goryachev, O. V. Borshchev, S. A. Ponomarenko, V. F. Razumov, N. S. Sariciftci, unpublished.
[30] S. Wakim, S. Beaupre, N. Blouin, B.-R. Aich, S. Rodman, R. Gaudiana, Y. Tao, M. Leclerc, *J. Mater. Chem.* **2009**, *19*, 5351.
[31] T.-Y. Chu, S. Alem, S.-W. Tsang, S.-C. Tse, S. Wakim, J. Lu, G. Dennler, D. Waller, R. Gaudiana, Y. Tao, *Appl. Phys. Lett.* **2011**, *98*, 253301.
[32] N. Blouin, A. Michaud, D. Gendron, S. Wakim, E. Blair, R. Neagu-Plesu, M. Belletete, G. Durocher, Y. Tao, M. Leclerc, *J. Am. Chem. Soc.* **2008**, *130*, 732.
[33] N. Blouin, A. Michaud, M. Leclerc, *Adv. Mater.* **2007**, *19*, 2295.
[34] J. C. Hummelen, B. W. Knight, F. Lepeq, F. Wudl, J. Yao, C. L. Wilkins. *J. Org. Chem.* **1995**, *60*, 532.
[35] J. Y. Mayorova, S. L. Nikitenko, P. A. Troshin, S. M. Peregudova, A. S. Peregudov, M. G. Kaplunov, R. N. Lyubovskaya. *Mendeleev Commun.* **2007**, *17*, 175.
[36] P. A. Troshin, E. A. Khakina, M. Egginger, A. E. Goryachev, S. I. Troyanov, A. Fuchsbauer, A. S. Peregudov, R. N. Lyubovskaya, V. F. Razumov, N. S. Sariciftci, *ChemSusChem* **2010**, *3*, 356.
[37] P. A. Troshin, H. Hoppe, J. Renz, M. Egginger, J. Y. Mayorova, A. E. Goryachev, A. S. Peregudov, R. N. Lyubovskaya, G. Gobsch, N. S. Sariciftci, V. F. Razumov, *Adv. Funct. Mater.* **2009**, *19*, 779.